Supplementary information for:

Nanoscale spatial dependence of avidity in an IgG1 antibody

Agnieszka Jendroszek,[1,2] and Magnus Kjaergaard[1-4*]

[1] Department of Molecular Biology and Genetics, Aarhus University

[2] The Danish Research Institute for Translational Neuroscience (DANDRITE)

[3] Aarhus Institute of Advanced Studies (AIAS)

[4] The Center for Proteins in Memory (PROMEMO)

[*] Corresponding author: magnus@mbg.au.dk

Sequences of APH constructs

Color code:

His-tag Thrombin site *Flexible linker*

APH_{half}

MGSS**HHHHHH**SSGMKQLEKELKQLEKELQAIEKQLAQLQKKAQARKKKLAQLKKKLQA*PGSGSGP*MKQL EKELKQLEKELQAIEKQLAQLQWKAQARKKKLAQLKKKLQA

APH_{4}

MGSS**HHHHHH**SSGMKQLEKELKQLEKEAQARKWKLAQLKKKLQA

$APH_{4\_thrombin}$

MGSS**HHHHHH**SSGLVPRGSHMKQLEKELKQLEKEAQARKWKLAQLKKKLQA

APH_{6}

MGSS**HHHHHH**SSGMETKQLEKELKQLEKELQAIEKQLAQLQWKAQARKKKLAQLKKKLQA

$APH_{6\_thrombin}$

MGSS**HHHHHH**SSGLVPRGSHMKQLEKELKQLEKELQAIEKQLAQLQWKAQARKKKLAQLKKKLQA

APH_{8}

MGSS**HHHHHH**SSGMKQLEKELKQLEKELQAIEKQLAQLQKKLQAIEKQLAQLQWKAQARKKKLAQLKKK LQA

$APH_{8\_thrombin}$

MGSS**HHHHHH**SSGLVPRGSHMKQLEKELKQLEKELQAIEKQLAQLQKKLQAIEKQLAQLQWKAQARKKK LAQLKKKLQA

APH_{10}

MGSS**HHHHHH**SSGMKQLEKELKQLEKELQAIEKQLAQLQKKAQARKKKLKQLEKELQAIEKQLAQLQWK AQARKKKLAQLKKKLQA

$APH_{10\_thrombin}$

MGSS**HHHHHH**SSGLVPRGSHMKQLEKELKQLEKELQAIEKQLAQLQKKAQARKKKLKQLEKELQAIEKQL
AQLQWKAQARKKKLAQLKKKLQA

APH_{12}

MGSS**HHHHHH**SSGMKQLEKELKQLEKELQAIEKQLAQLQKKAQARKKKLAQLKKKLQALEKELKQLEKE
LQAIEKQLAQLQWKAQARKKKLAQLKKKLQA

$APH_{12\_thrombin}$

MGSS**HHHHHH**SSGLVPRGSHMKQLEKELKQLEKELQAIEKQLAQLQKKAQARKKKLAQLKKKLQALEKE
LKQLEKELQAIEKQLAQLQWKAQARKKKLAQLKKKLQA

APH_{16}

MGSS**HHHHHH**SSGMKQLEKELKQLEKELQAIEKQLAQLQKKAQARKKKLQALEKELKQLEKELQAIEKQL
AQLQKKAQARKKKLAQLKKKLKQLEKELQAIEKQLAQLQWKAQARKKKLAQLKKKLQA

$APH_{16\_thrombin}$

MGSS**HHHHHH**SSGLVPRGSHMKQLEKELKQLEKELQAIEKQLAQLQKKAQARKKKLQALEKELKQLEKEL
QAIEKQLAQLQKKAQARKKKLAQLKKKLKQLEKELQAIEKQLAQLQWKAQARKKKLAQLKKKLQA

APH_{18}

MGSS**HHHHHH**SSGMKQLEKELKQLEKELQAIEKQLAQLQKKAQARKKKLAQLKKKLQALEKELKQLEKE
LQAIEKQLAQLQKKAQARKKKLAQLKKKLQALEKELKQLEKELQAIEKQLAQLQWKAQARKKKLAQLKKK
LQA

$APH_{18\_thrombin}$

MGSS**HHHHHH**SSG*LVPRGS*HMKQLEKELKQLEKELQAIEKQLAQLQKKAQARKKKLAQLKKKLQALEKEL
KQLEKELQAIEKQLAQLQKKAQARKKKLAQLKKKLQALEKELKQLEKELQAIEKQLAQLQWKAQARKKKL
AQLKKKLQA

APH_{20}

MGSS**HHHHHH**SSGMKQLEKELKQLEKELQAIEKQLAQLQKKAQARKKKKQLEKELQAIEKQLAQLQKKA
QARKKKLAQLKKKLQALEKELKQLEKELQAIEKQLAQLQKKAQARKKKLKQLEKELQAIEKQLAQLQWKA
QARKKKLAQLKKKLQA

$APH_{20\_thrombin}$

MGSS**HHHHHH**SSG*LVPRGS*HMKQLEKELKQLEKELQAIEKQLAQLQKKAQARKKKQLEKELQAIEKQLA
QLQKKAQARKKKLAQLKKKLQALEKELKQLEKELQAIEKQLAQLQKKAQARKKKLKQLEKELQAIEKQLA
QLQWKAQARKKKLAQLKKKLQA

APH_{24}

MGSS**HHHHHH**SSGMKQLEKELKQLEKELQAIEKQLAQLQKKAQARKKKLAQLKKKLQALEKELKQLEKE
LQAIEKQLAQLQWKAQARKKKLAQLKKKLQALEKELKQLEKELQAIEKQLAQLQKKAQARKKKLAQLKKK
LQALEKELKQLEKELQAIEKQLAQLQWKAQARKKKLAQLKKKLQA

$APH_{24\_thrombin}$

MGSS**HHHHHH**SSG*LVPRGS*MKQLEKELKQLEKELQAIEKQLAQLQKKAQARKKKLAQLKKKLQALEKELK
QLEKELQAIEKQLAQLQWKAQARKKKLAQLKKKLQALEKELKQLEKELQAIEKQLAQLQKKAQARKKKLA
QLKKKLQALEKELKQLEKELQAIEKQLAQLQWKAQARKKKLAQLKKKLQA

Table S1. Kinetic constants determined by SPR for APH variants binding to THE His Ab.

		BIACORE evaluation software				IGOR Pro	
pH		k_{on1} $10^3 \times (Ms)^{-1}$	k_{off1} (ms^{-1})	k_{on2} $10^{-4} \times (Ms)^{-1}$	k_{off2} (ms^{-1})	k_{off1} (ms^{-1})	k_{off2} (ms^{-1})
5.8	APH_4	225.9 ± 2.4	19.2 ± 0.1	n.d.	n.d.	n.d.	n.d.
	APH_6	95.8 ± 0.5	18.5 ± 0.2	2.74 ± 0.02	0.80 ± 0.01	22.6 ± 1.3	1.1 ± 0.12
	APH_8	76.7 ± 0.4	13.7 ± 0.2	1.63 ± 0.02	0.63 ± 0.02	18.9 ± 1.0	0.78 ± 0.10
	APH_{10}	122.5 ± 0.2	14.8 ± 0.1	2.39 ± 0.01	0.66 ± 0.01	19.5 ± 1.1	0.70 ± 0.068
	APH_{12}	100.8 ± 0.4	19.9 ± 0.2	1.74 ± 0.01	0.62 ± 0.01	19.6 ± 1.1	0.60 ± 0.050
	APH_{16}	29.0 ± 0.3	20.8 ± 0.6	0.94 ± 0.02	0.77 ± 0.03	16.7 ± 1.4	0.74 ± 0.14
	APH_{18}	47.7 ± 0.3	19.5 ± 0.3	1.16 ± 0.01	1.26 ± 0.02	20.9 ± 1.7	1.5 ± 0.16
	APH_{20}	104.4 ± 0.3	15.5 ± 0.2	1.88 ± 0.02	1.22 ± 0.01	17.4 ± 1.2	1.2 ± 0.095
	APH_{24}	65.2 ± 0.4	21.4 ± 0.4	1.08 ± 0.01	1.48 ± 0.02	17.0 ± 1.2	1.3 ± 0.15
	APH_{half}	54.6 ± 1.4	18.5 ± 0.1	n.d.	n.d.	n.d.	n.d.
6.0	APH_{12}	38.7 ± 0.3	4.30 ± 0.13	0.54 ± 0.01	0.18 ± 0.003	6.5 ± 0.6	0.17 ± 0.0135
	APH_{half}	118.8 ± 0.5	8.61 ± 0.06	n.d.	n.d.	n.d.	n.d.
6.2	APH_{12}	66.9 ± 0.1	3.76 ± 0.02	0.72 ± 0.004	0.11 ± 0.001	3.8 ± 0.3	0.074 ± 0.0085
	APH_{half}	152.7 ± 0.7	6.22 ± 0.02	n.d.	n.d.	n.d.	n.d.

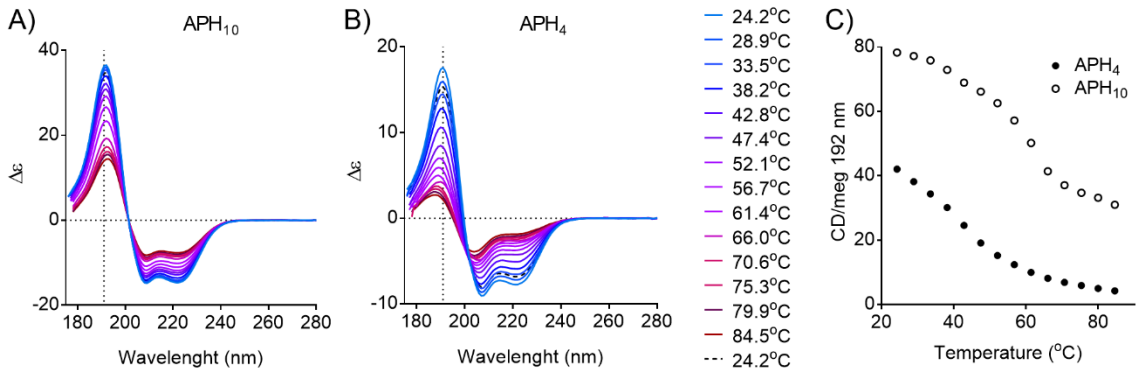

Figure S1. SR-CD spectra of APH_{10} (A) and APH_4 (B) were measured at temperatures varying from 25°C to 85°C. Dotted line indicates 192 nm the wavelength at which change of the CD signal intensity with temperature was compared (C).

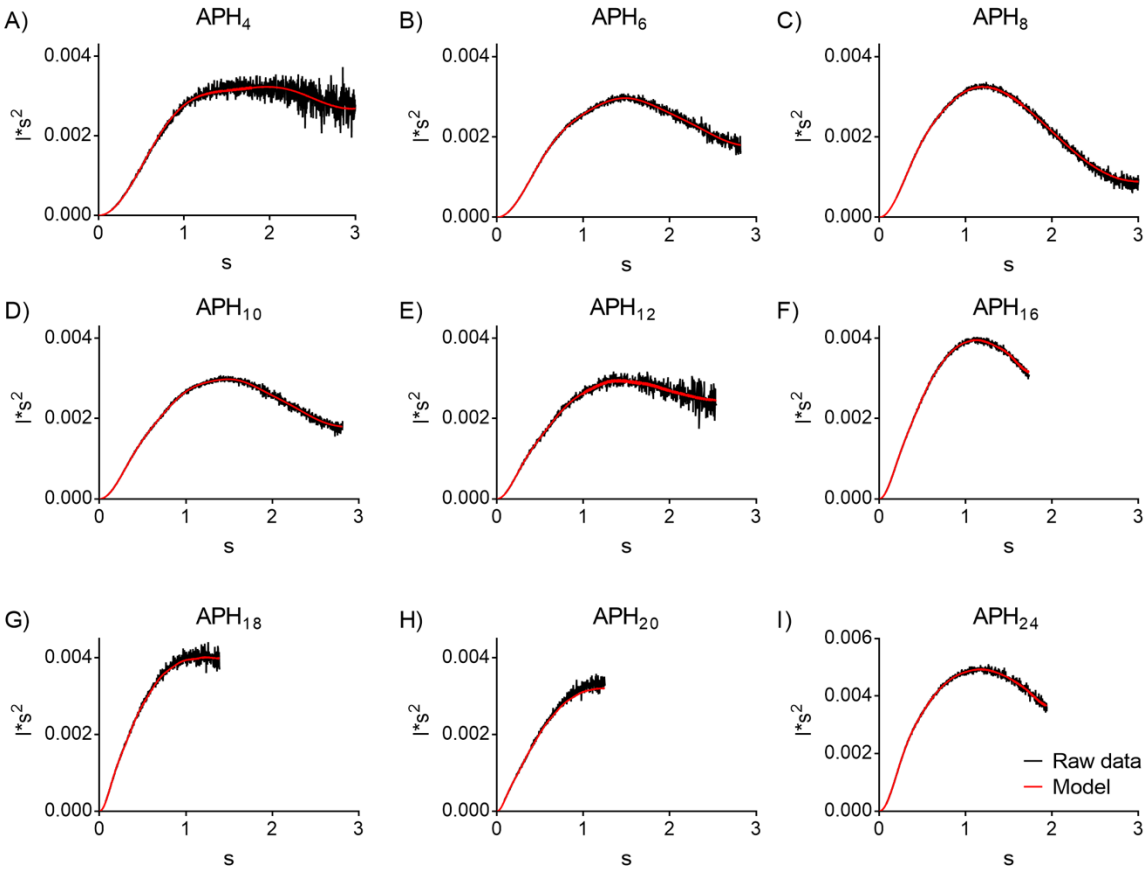

Figure S2. SAXS data of all APH variants represented as Kratky plots.

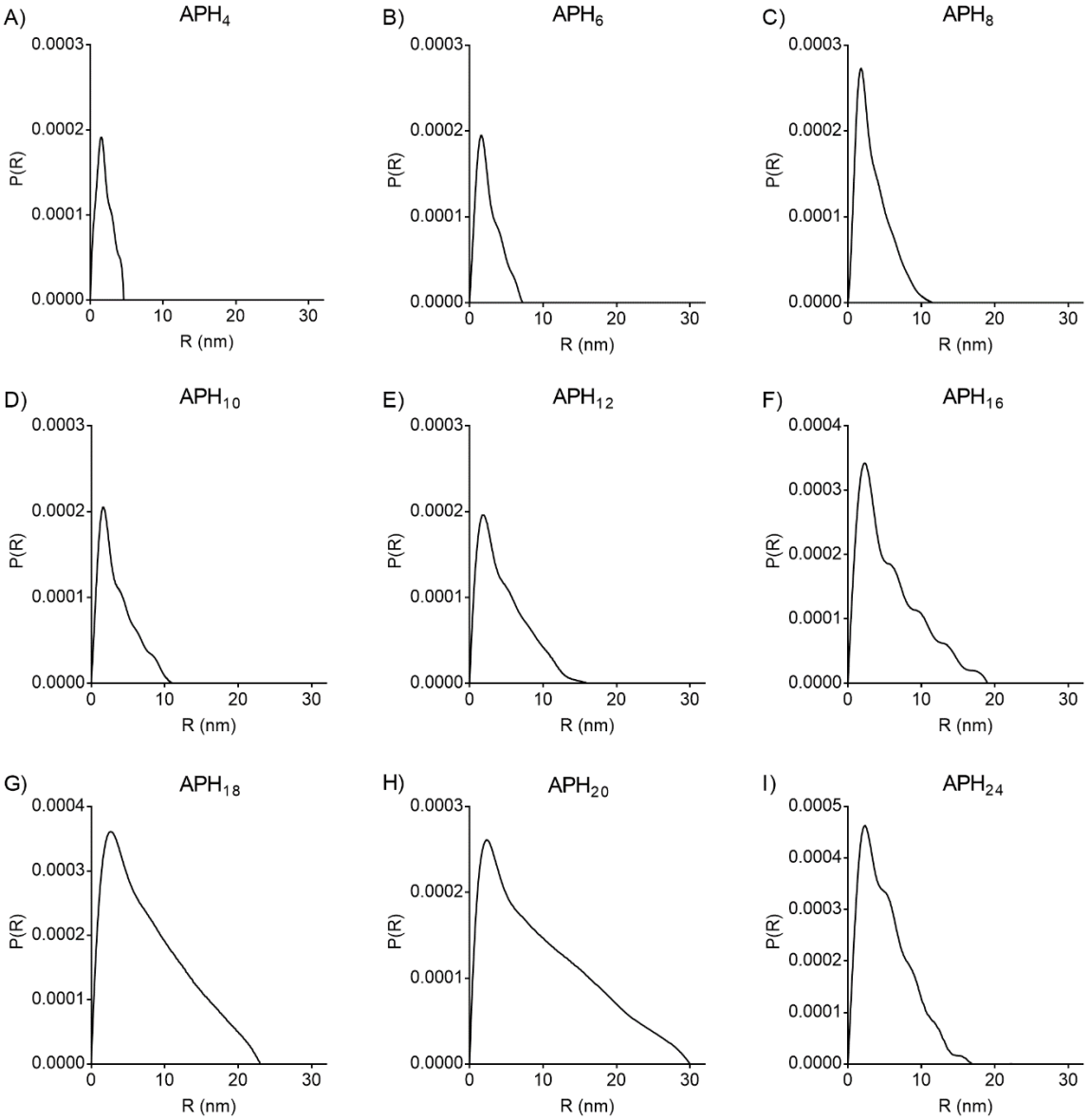

Figure S3. SAXS data for all variants represented as p(r) functions. The maximum distance (D_{max}) increases steadily up to APH_{18}, whereafter it dramatically increase in APH_{20} and is reduced in APH_{24}. These data mirror the R_g and the R_h determined from DLS.

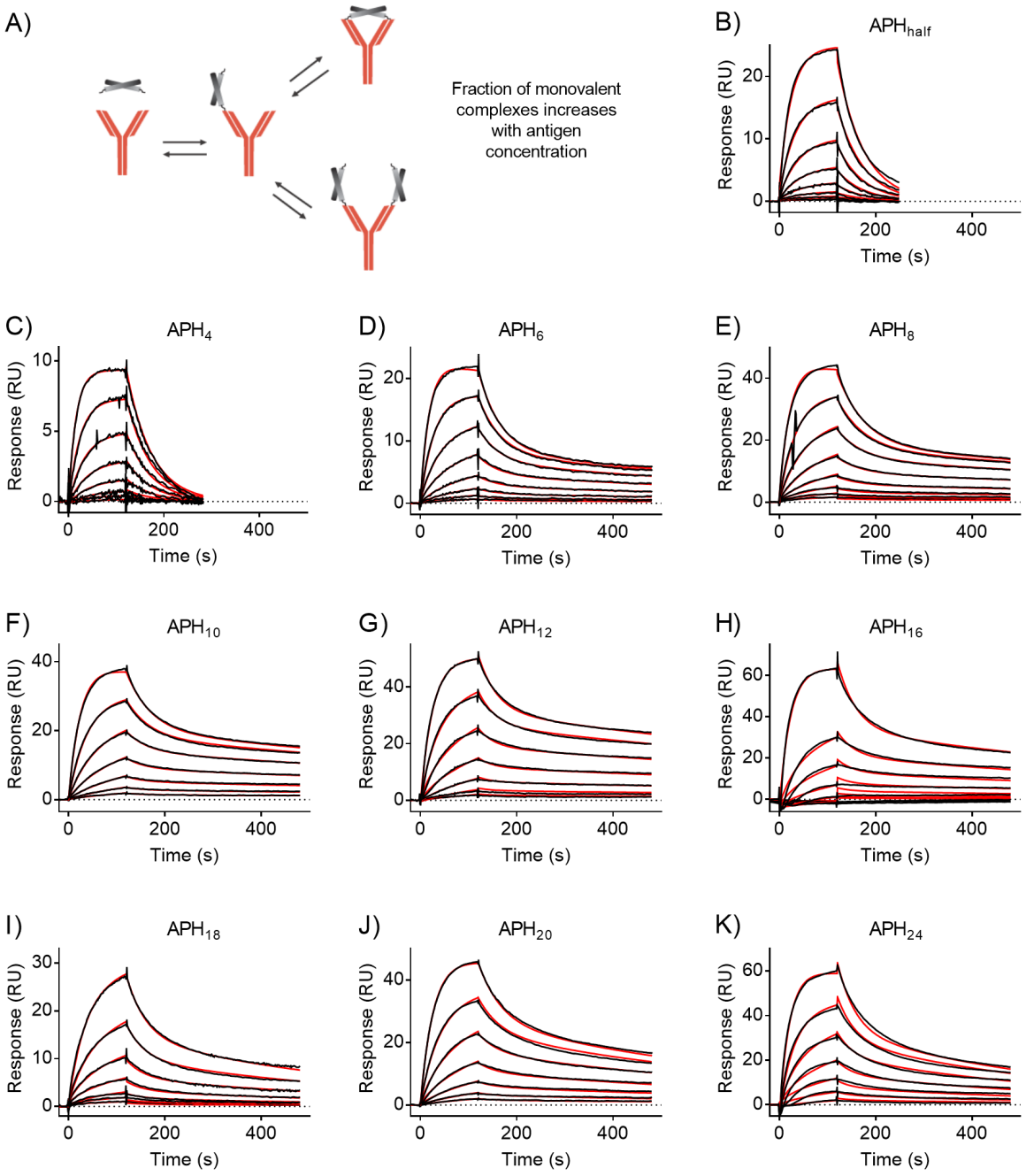

Figure S4. Binding of a bivalent antigen to an antibody can result in formation of mono- and bivalent complexes (A). Fraction of antigens interacting with an antibody via single epitope increases with the antigen concertation. Representative sensorgrams of all antigens binding to anti-His antibody at pH 5.8 are shown in (B) to (K). Black lines refer to raw data and 1:1 (APH_{half}, APH_4) or bivalent analyte (APH_6, APH_{10}, APH_{12}, APH_{16}, APH_{18}, APH_{20}, APH_{24}) fit is shown as red lines.

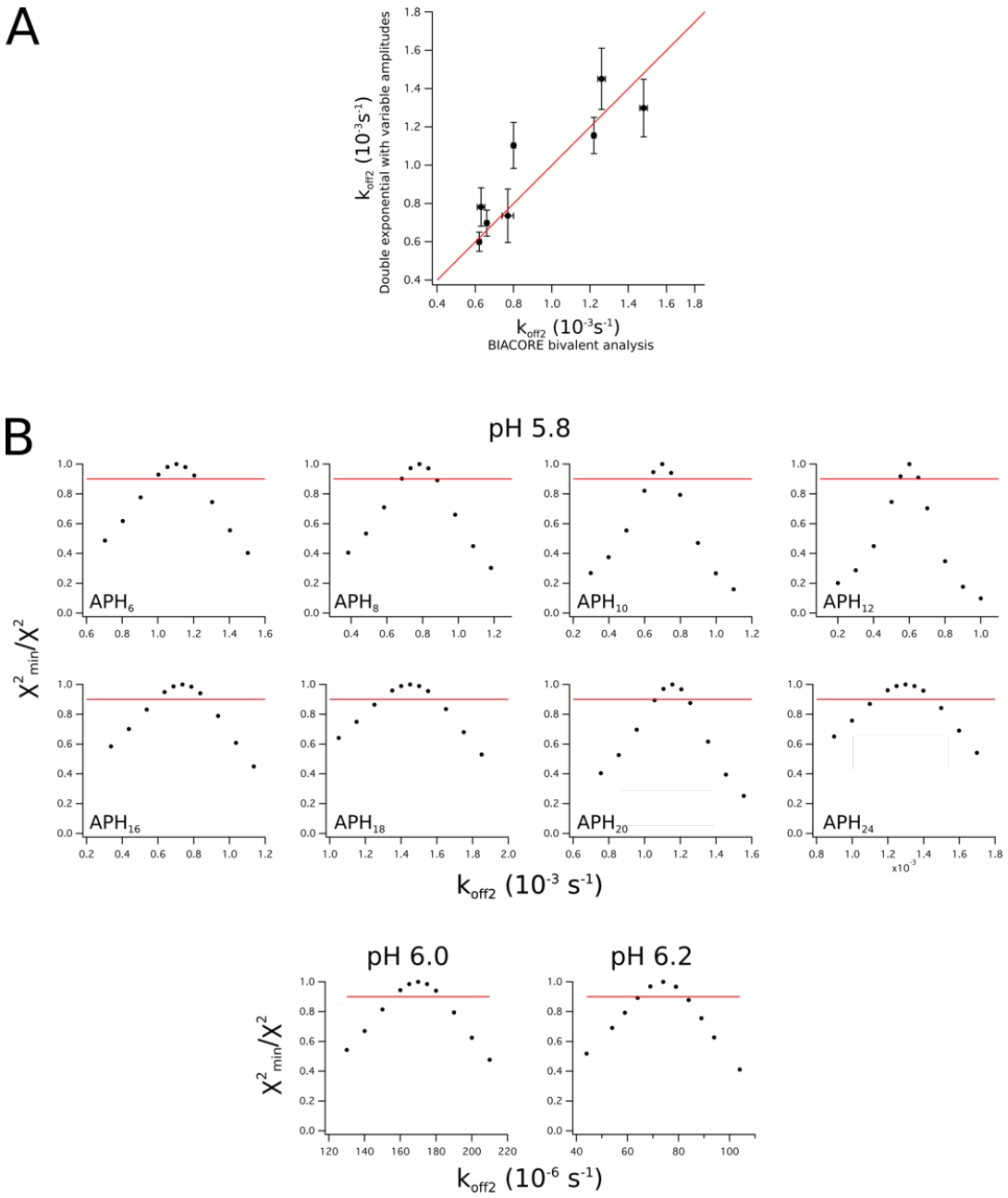

Figure S5. Confidence analysis of dissociation rate constants. A) The SPR data were either analysed by fitting the full data set to bivalent model in the BIACORE Evaluation software, resulting in adequate fits. We also fit the dissociation phase to a double exponential, where the amplitudes vary freely but the two rate constants are fitted globally, which improves the fit. B) To evaluate the confidence interval of the fitted rate constants, we evaluated the χ^2-curves using the bivalent fit by locking k_{off2} to values around the fitted value and fitting the remaining parameters. All the fitted parameters are located in well-defined χ^2 minima, suggesting they are well determined by the data. Built-in error estimations typically underestimate the error associated with co-variance between fitted variables, and therefore we determined the confidence interval from a threshold of $\chi^2_{min}/\chi^2 = 0.9$ (red line) following the criteria defined by Johnson et al. (Ref. 37 in main manuscript)